Sustainable Energy, Grids and Networks

A Customised Artificial Neural Network for Power Distribution System Fault Detection

--Manuscript Draft--

Manuscript Number:	SEGAN-D-23-00789
Article Type:	Research Paper
Keywords:	Customised artificial neural network; power system faults; IEEE-33 bus distribution system; Typhoon HIL; sustainaibility
Corresponding Author:	Soham Dutta, Phd Manipal Institute of Technology INDIA
First Author:	ARNAV BHAGWAT
Order of Authors:	ARNAV BHAGWAT
	Soham Dutta, Phd
	VINAY KUMAR JADOUN, Phd
	Arigela Sri Satya Veerendra Babu, Phd
	Sourav Kumar Sahu
Abstract:	The occurrence of faults poses a constant threat to the distribution grid operation. The faults occurring in these distribution grids are dangerous and unpredictable. The penetration of renewable based distributed generators (DGs) has further complicated the process of these fault detections. Hence, following the aims of Sustainable Development Goal 7, i.e. to guarantee access to reliable modern energy for all, a fast and accurate fault detection methodology needs to be developed. In this regard, a customised artificial neural network (CANN) for fault detection in a distribution grid is proposed in this paper. The data needed to train the model has been taken from a reconfigured IEEE-33 bus distribution system developed in Typhoon HIL real-time simulator. Spectral-kurtosis is utilized for extraction of features of the faulted transient signals which are used as input data to develop a CANN. For better capability of the procedure, optimized feature importance values are considered. The authors have considered other machine learned techniques to showcase a comparative study with the CANN.
Suggested Reviewers:	DEBAYAN SARKAR, PHD debayansarkar92@gmail.com Expert in neural network and renewable energy
	ANIK GOSWAMI, PHD Assistant Professor, Vellore Institute of Technology - Chennai Campus anik.goswami52@gmail.com Proficient in renewable energy and neural network
	BALMIDI MALLIKARJUNA, PHD Assistant Professor, National Institute of Technology Silchar arjun.malli4@gmail.com Expert in fault analysis in microgrid
	SAJJAN Kumar, PHD Assistant Professor, SSN Trust sajjan.pradhan48@gmail.com Expert in soft computing
	BISHWAJIT DEY, PHD Assistant Professor, Adani University sonu.aec2007@gmail.com Expert in neural network and microgrid
	MILLEND ROY Microsoft Research India millendroy239@gmail.com

	Proficient in fault analysis in microgrid
Opposed Reviewers:	

A Customised Artificial Neural Network for Power Distribution System Fault Detection

[1]Arnav Bhagwat, [1*]Soham Dutta, [1]Vinay Kumar Jadoun, [1]Arigela Sri Satya Veerendra Babu, [2]Sourav Kumar Sahu

[1]Department of Electrical and Electronics Engineering, Manipal Institute of Technology, Manipal Academy of Higher Education, Manipal, Karnataka, 576104, India
[2]Engineer, Magna Steyr India, A division of Magna Automotive India Private Limited, Pune, 411021, India

* soham.dutta@manipal.edu

Abstract: The occurrence of faults poses a constant threat to the distribution grid operation. The faults occurring in these distribution grids are dangerous and unpredictable. The penetration of renewable based distributed generators (DGs) has further complicated the process of these fault detections. Hence, following the aims of Sustainable Development Goal 7, i.e. to guarantee access to reliable modern energy for all, a fast and accurate fault detection methodology needs to be developed. In this regard, a customised artificial neural network (CANN) for fault detection in a distribution grid is proposed in this paper. The data needed to train the model has been taken from a reconfigured IEEE-33 bus distribution system developed in Typhoon HIL real-time simulator. Spectral-kurtosis is utilized for extraction of features of the faulted transient signals which are used as input data to develop a CANN. For better capability of the procedure, optimized feature importance values are considered. The authors have considered other machine learned techniques to showcase a comparative study with the CANN.

Keywords: Customised artificial neural network, power system faults, IEEE-33 bus distribution system, Typhoon HIL, sustainaibility

1. Introduction

The tech-based society is now being increasingly dependent on electricity and its related applications. Almost all the equipment in the households are run with electricity which simplifies the task and aids in saving time in our busy lives. Thus, electricity has become an integral part of human life. This has triggered a competitive environment among the electrical power providers in terms of continuity and reliability of power service [1]. For this, the power operators need to avoid power system faults and its related outages as quickly as possible to decrease the impact on the consumers [2].

Fault occurs in a distribution system when any two phases or all the phases of the distribution line come in contact with each other either solidly or through physical structures like branch of trees, birds, etc. When it occurs, there is a deviation from the normal operating conditions of the distribution grid. Out of these faults, some faults are short lived and normal conditions are retrieved after a short time interval. These faults, termed as temporary faults, do not possess problems in general [3]. However, some faults are permanent and are not cleared automatically. Disruptions of the distribution line leading to physical contact with the earth, insulation failure of the power cables, sagging, etc., are some of the permanent faults. These faults need to be recognized and removed by the power protection engineers as soon as possible to maintain the power reliability. Out of all the power system outages instants, faults contribute almost three-fourth of it [4].

1.1 Impetus of the research

The traditional distribution system had a smaller geographical span. The components used in it were simple and managing the power flow was easier due to its unidirectional nature [5]. Hence, any occurrence of fault did not exhibit a major problem as they were easier to detect as well as locate. The fault could be easily located by conventional approaches such as trial and error switching, manual inspection, etc. Even the protection equipment in some advanced distribution grids had a simple algorithm for fault detection and had a very minimal chance of nuisance tripping. As technology progressed, the distribution system got increasingly complexed. The economical as well as population growth also led to an expand in the geographical extent of the distribution power system. The modern distribution system paradigm has a bidirectional power flow due to the penetration of distributed energy resources triggered by the introduction of various national and international policies such as Sustainable Development Goal 7 [6]. Thus, owing to the increase in geographical sprawl and intricacies of the distribution system, the traditional fault detection approaches will not work. Hence, all the protection algorithms and devices need to be upgraded to ensure power continuity to the modern consumers.

The modern distribution grid is equipped with advanced meters such as phasor measurement units, smart meters, etc [7]. These instruments measure and record data at a high accuracy and in high volume. These high voluminous data can cater to the need of developing an algorithm for fault detection in a complex distribution grid. Embracing the era of artificial intelligence, a customised machine learned (ML) fault detection approach can be developed to detect and classify faults in power distribution system.

1.2 Previously published papers related to fault detection

The previously published work on fault detection technologies can be categorised into two divisions- traditional and modern methods. The traditional methods deal with simple approaches such as impedance calculation, travelling waves, etc. The modern methods can further be divided into phasor measurement units-based methods, signal processing methods, knowledge-based methods and ML based methods. The basic principle of working and the different variations of each technique is explained in the subsequent sections.

The travelling wave technique work uses the principle of transmission and reflection of travelling waves in between the line terminal and location of the fault. For an uni-terminal network, the velocity and time of the travelling wave are calculated for estimating the fault location in [8]. For a bi-terminal network, a real time fault location is estimated based on travelling wave and a communication system. In impedance-based techniques, the impedance between the fault location and a specific measurement location is calculated for estimation of faults. In [10], the imaginary portion of the impedance is compared against the reactance of the line for detecting faults. In [11], a direct method is presented which utilizes the admittance matrix, fault admittance matrix and the load impedance matrix for estimation of faults. The conventional methods are simple but suffers inadequate classification ability and slower detection time for complex distribution systems.

The phasor measurement units-based technique employs synchrophasors for detecting fault at various locations by exploiting the current and voltage phasors obtained from the phasor measurement units. The Thevenin equivalent of zero sequence, positive sequence and negative sequence for different source types is calculated in [12] from the synchrophasor data to detect fault. The difference in magnitude of the change of voltage phase angle with time between the fault location and point of common coupling of a microgrid is estimated with phasor measurement units and is used for fault detection in [13]. These methods have an advantage of high accuracy but have huge capital costs. Besides, these methods rely on communication channel and reference phasors which may get disrupted during catastrophize or cyber-attack.

The last few decades witnessed the growth in use of signal processing techniques and pattern recognition methods in the field of fault detection. The methodology behind these techniques involve measuring the fault related signals such as voltage, current, etc. and analysing the signals with advanced signal processing methods for obtaining some features or for a clear representation of signals. A fault detection method based on cumulative sum of wavelet transform features is explained in [14]. A Stockwell transform based differential fault detection and classification approach is dealt in [15, 16]. PSCAD and MATLAB software is used to simulate fault conditions in IEEE 14 bus system and WSCC 9 bus system and to develop a Hilbert Hwang transform based fault detection methodology in [17]. Mathematical morphology-based fault detection method is presented in [18]. These methods are helpful to visualize the fault signals in a better way. However, determination of the thresholds for classification of the faults become difficult for large systems.

The last few years have seen a rapid increase in the computing power of the machines. This has led to an increase in the usage of computer aided knowledge-based methods of fault detection. The most well-known knowledge-based method is the fuzzy logic method which employs the idea of possibility in stead of probability. The higher order statistics are developed in [19] to probe the fault signal characteristics for classifying by using fuzzy logic. The line currents of all the phases are measured in [20] and are analysed with fuzzy logic for the determination of type of fault. [21] is an extended version of [20] where unbalanced network is considered for fault classification. An automated program flow and control methodology with the application of fuzzy logic for classification of faults is presented in [22]. These methods have the advantage of high accuracy but have a disadvantage of huge dependence on the knowledge of an experienced professional.

The shortcomings of the above-mentioned methods have fuelled the usage of ML techniques for detection and classification of different types of faults occurring in power distribution system. These techniques are recently being applied in power system sector in an exponential manner. In these methods, a model is first learned by training it with various input and output features and then it is used to categorise testing data into different categories. The accuracy is then obtained based on the number of instants of correct identification of test data. An artificial neural network (ANN) is trained to aid the operators in identifying faulty section in [23]. In [24], ANN is trained for identifying high impedance faults. The authors in [25] has used a multilayer perceptron neural network for recognizing different faults and its location. Wavelet transform is used along with modular multilayer feed forward neural network for fault identification in [26]. The fundamental components of current and voltage signal are used to train a support vector machine (SVM) in [27] for unhealthy phases for estimating fault location. SVM along with radial basis neural network is used in [28] for identifying fault from voltage signals. Wavelet transform with SVM is used in [29, 30] to find fault location. A real time algorithm is developed in [31] that uses mathematical morphology with decision tree (DT) for identification and classification of faults. Instantaneous values of normalised currents of all phases are used in [32] to train a k-nearest neighbour (KNN) classifier for fault detection. For the application of ML classifiers in fault detection, generally, the power system researchers ignore the underlying architecture of these ML model. This removes the scope of further improvement in the accuracy of the ML algorithms. Thus, the knowledge of a detailed step by step building of any ML classifier in needed for making room for some possible increase in accuracy.

The performance of an ANN is affected by its architecture. In fact, obtaining the optimum number of hidden layers and their nodes is the biggest challenge in building a network. The present algorithm aims at addressing this above problem. A customised ANN (CANN) model is developed as per the requirement for fault classification and finding its location rather than using an available ANN model as a black box. The data needed to train the model has been taken from a reconfigured IEEE-33 bus distribution system developed in Typhoon HIL real-time simulator [33]. Spectral-kurtosis is utilized for extraction of features of the faulted transient signals which are used to as input data to develop a CANN. The customisation results in an increase of accuracy and a better understanding of the underlying architecture of CANN.

1.3 Features of the work

The features of the present work in comparison to other works in the field of fault detection are as follows:

- A CANN model is developed as per the requirement for fault classification and finding its location rather than using an available ANN model as a black box.
- The method of obtaining the optimum number of hidden layers and their nodes of CANN is explained to understand the architecture.
- The method of reducing the input features of CANN to improve the accuracy is stated.
- Real time data are used to train the model to eradicate the errors of simulation data.
- The accuracy of the CANN is higher than the other ML techniques.

1.4 Organisation of the work

The rest of the paper is organized as follows. Section 2 deals with the test system and a brief detail about the dataset. Section 3 deals with the methodology to develop the CANN where processing and partitioning of the data is explained. The specifications of the customised model and its improvement by reducing the number of input features is also explained in this section. The performance and the results of the CANN is dealt in Section 4. The comparison of the present model with other classifier models is discussed in this section. The last section of the paper concludes the present work.

2. Test System and Dataset

The test system consists of an IEEE 33 node distribution test system. The traditional system is modified to transform it into in active distribution network as shown in Figure 1. Three solar distributed generators (DGs) are added to the system, at node 14, 24 and 29. For obtaining results from this network in a real-time stage, “configuration 2” in Typhoon HIL602+ device is taken for maximum utilization of FPGA cores. Several fault types at various locations with various fault resistances are introduced and the high-resolution data obtained from the real-time simulation is logged. The data obtained are voluminous as 2 million samples from the internal signal scope of the simulator is obtained per second. The whole model is explained in detail in [33].

As the fault signals inherently possess a non-stationary character, spectral kurtosis has been executed on the current signals and several features have been derived to study the fault characteristics. The theory of spectral kurtosis and the procedure to obtain the features are explained in detail in [33]. To train and test the proposed ANN, numerous data samples of different transients that appear as faults are analysed, along with the position where these faults occur. A portion of the dataset is shown in Figure 2. The three phase currents obtained during the fault are represented by IA, IB and IC respectively. The subdivisions under each phase currents are the value of spectral kurtosis obtained from this signal at different normalised frequency. These parts serve as the input matrix for the ML models. As shown by the dataset, there are 10 different types of faults that are observed (AB, ABN, AC, etc.). Similarly, the dataset shows that each fault can occur at 28 different possible bus locations in the sampled system. These sections serve as the output matrix for the ML models. Thus, an ANN model is developed that has 30 input features and10 different output classes when classifying fault type and 28 different classes when classifying fault location. A total of 1800 test samples were generated, wherein 80% of the samples were used for training the model and 20% of the data was used for testing the model. The ANN designed to solve fault type and fault location is a custom designed artificial network that takes in the chosen features and makes predictions based on the data it is fed.

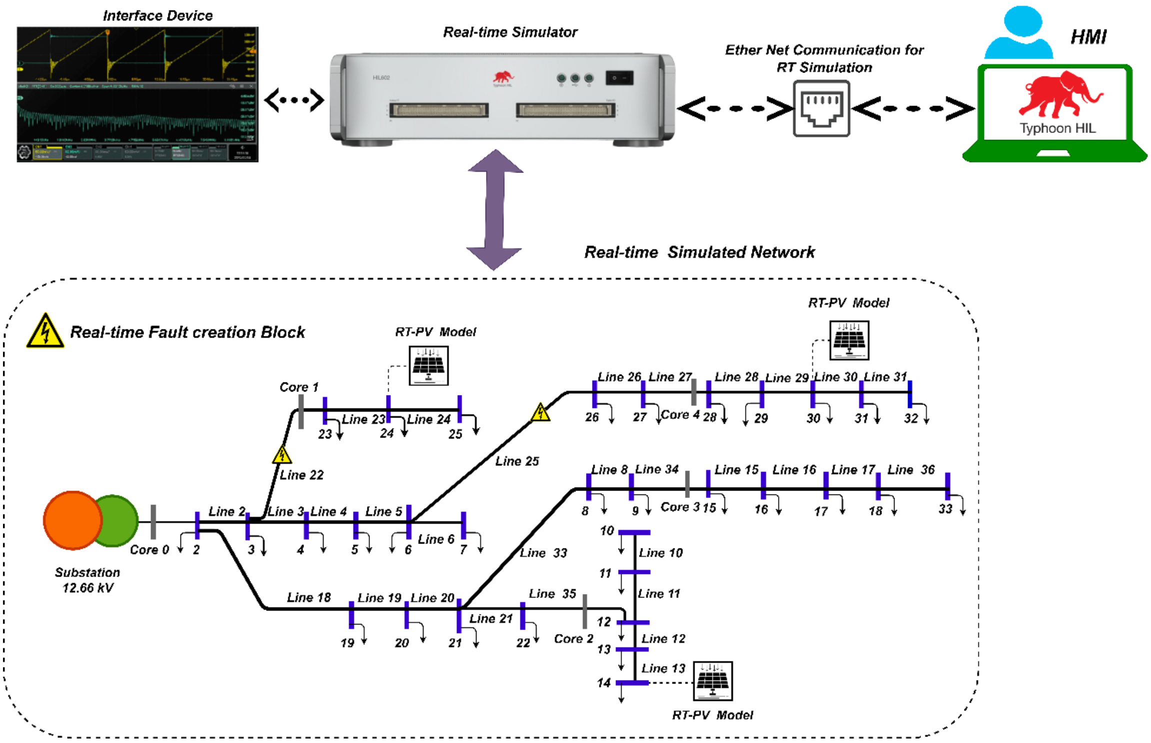

Figure 1: Test system considered

IA										IB										IC										FLT	Position	Key
-0.61679	-0.65755	-0.6983	-0.80019	-0.75943	-0.73566	-0.88509	-0.83755	-0.57604	0.001321	-0.629433962	-0.6566	-0.66264	-0.80151	-0.75925	-0.70792	-0.84377	-0.82566	-0.56302	-0.09509	0.0292	-0.6047	-0.7745	-0.8991	-0.9613	-0.9104	-0.6953	-0.3047	-0.3443	-0.95	AB	19-20	0
-0.6439	-0.6099	-0.6495	-0.7882	-0.7571	-0.7203	-0.9156	-0.8844	-0.5703	-0.092	-0.6592	-0.6389	-0.6208	-0.777	-0.7589	-0.7408	-0.9513	-0.9083	-0.5596	-0.7045	-0.6108	-0.5967	-0.6108	-0.7665	-0.7524	-0.7335	-0.8467	-0.9505	-0.5825	0.6344	ABC	19-20	0
-0.6389	-0.58	-0.6434	-0.7838	-0.7566	-0.7294	-0.9083	-0.7928	-0.5913	-0.6592	-0.6134	-0.6425	-0.653	-0.7877	-0.7587	-0.7191	-0.8802	-0.8353	-0.55	-0.5791	1037.9	-1.3	2.1	2.1	97.2	-1.3	-1.3	-1.3	-1.3	1547.4	ABN	19-20	0
-0.6213	-0.6504	-0.6926	-0.8115	-0.7534	-0.7402	-0.8538	-0.9172	-0.5738	-0.476	0.1481	-0.5934	-0.8142	-0.9047	-0.9613	-0.9104	-0.6557	-0.3726	-0.4406	-0.9104	-0.6156	-0.6495	-0.6807	-0.7995	-0.7571	-0.7542	-0.8448	-0.8703	-0.5675	-0.208	AC	19-20	0
-0.623	-0.6072	-0.6638	-0.7974	-0.7543	-0.7091	-0.8585	-0.8653	-0.5823	-0.6298	1054.9	-1.3	-1.3	-1.3	117.5	-1.3	-1.3	-1.3	-1.3	1550.8	-0.623	-0.6796	-0.7113	-0.7838	-0.7521	-0.743	-0.8811	-0.9558	-0.5777	-0.7045	ACN	19-20	0
-0.6525	-0.6909	-0.7136	-0.8019	-0.7566	-0.7272	-0.8811	-0.8834	-0.5755	-0.6751	0.6981	0.0189	-0.2075	-0.434	-0.5094	-0.434	-0.283	-0.0566	0.1698	-0.8113	-0.466	-0.6472	-0.734	-0.8321	-0.7981	-0.7679	-0.9226	-0.7906	-0.4925	-0.9264	AN	19-20	0
0.1142	-0.5934	-0.8085	-0.9047	-0.9557	-0.9047	-0.6953	-0.333	-0.384	-0.9783	-0.6363	-0.6628	-0.6735	-0.785	-0.7531	-0.7584	-0.8752	-0.7637	-0.6044	-0.6204	-0.6213	-0.7085	-0.7058	-0.7957	-0.756	-0.7375	-0.8723	-0.8617	-0.587	-0.3096	BC	19-20	0
-0.5257	-0.4464	-0.4645	-0.5415	-0.503	-0.4713	-0.5868	-0.6004	-0.4419	-0.9649	-0.6319	-0.6557	-0.6953	-0.793	-0.7587	-0.7428	-0.8485	-0.7692	-0.587	-0.587	-0.623	-0.6706	-0.7385	-0.7521	-0.7521	-0.7611	-0.8494	-0.9219	-0.5777	-0.5777	BCN	19-20	0
898.7	-1.3	-1.3	-1.3	1119.4	-1.3	-1.3	-1.3	2.1	1520.2	-0.6002	-0.6319	-0.6609	-0.7719	-0.756	-0.7375	-0.8591	-0.793	-0.55	-0.3017	1465.8	29.2	63.2	22.5	1530.4	104	36	70	416.4	1540.6	BN	19-20	0
1465.8	22.5	76.8	15.7	1533.8	80.2	25.8	56.4	396	1516.8	966.6	-1.3	-1.3	-1.3	1112.6	-1.3	-1.3	-1.3	-1.3	1544	-0.6451	-0.69	-0.7058	-0.7877	-0.7534	-0.7323	-0.904	-0.8591	-0.5817	-0.336	CN	19-20	0
-0.6198	-0.5972	-0.6765	-0.786	-0.7596	-0.7029	-0.8842	-0.8691	-0.5594	-0.8729	-0.6321	-0.6698	-0.6774	-0.7943	-0.7566	-0.734	-0.8736	-0.8321	-0.5491	-0.9038	-0.6909	-0.6819	-0.7136	-0.786	-0.7317	-0.7068	-0.854	-0.8585	-0.5709	-0.9423	AB	19-20	0
-0.6298	-0.6275	-0.6774	-0.7928	-0.7566	-0.7045	-0.8675	-0.9264	-0.5279	-0.8743	-0.6264	-0.6264	-0.6868	-0.8075	-0.7472	-0.7472	-0.8981	-0.7472	-0.566	-0.8679	-0.6396	-0.6245	-0.6698	-0.8094	-0.7566	-0.7189	-0.9	-0.7981	-0.5679	-0.6962	ABC	19-20	0
-0.6275	-0.6502	-0.6411	-0.7928	-0.7589	-0.7475	-0.8653	-0.8426	-0.5777	-0.9355	-0.5934	-0.6726	-0.6858	-0.8047	-0.7519	-0.7123	-0.884	-0.8443	-0.5538	-0.567	1292.6	-1.3	-1.3	-1.3	593	-1.3	-1.3	-1.3	5.5	1547.4	ABN	19-20	0
-0.6434	-0.6728	-0.6615	-0.7928	-0.7566	-0.7385	-0.8472	-0.897	-0.5664	-0.906	-0.6636	-0.6081	-0.6768	-0.7587	-0.7349	-0.7058	-0.8432	-0.8274	-0.6081	-0.97	-0.6266	-0.6213	-0.6821	-0.7772	-0.7587	-0.7402	-0.9092	-0.8696	-0.5923	-0.8908	AC	19-20	0
-0.6108	-0.5474	-0.6345	-0.7825	-0.7587	-0.7323	-0.8564	-0.8643	-0.5632	-0.9304	1316.4	-1.3	-1.3	-1.3	596.4	-1.3	-1.3	-1.3	8.9	1547.4	-0.6184	-0.6712	-0.7108	-0.7901	-0.7571	-0.7175	-0.8363	-0.7835	-0.5986	-0.5127	ACN	19-20	0
-0.6275	-0.5891	-0.6864	-0.7974	-0.7589	-0.7362	-0.8336	-0.8132	-0.58	-0.9513	-0.633	-0.667	-0.7236	-0.7915	-0.7689	-0.7406	-0.8934	-0.7972	-0.5425	-0.933	-0.6524	-0.5901	-0.6665	-0.7939	-0.7514	-0.7458	-0.8307	-0.8731	-0.5816	-0.9241	AN	19-20	0
-0.6557	-0.5606	-0.6187	-0.756	-0.7296	-0.7085	-0.8432	-0.8432	-0.5711	-0.9568	-0.6297	-0.6212	-0.6976	-0.7825	-0.7571	-0.7146	-0.9014	-0.842	-0.5618	-0.4344	-0.5906	-0.6358	-0.6811	-0.8283	-0.7604	-0.7151	-0.8736	-0.8283	-0.5906	-0.3302	BC	19-20	0
-0.5438	-0.5823	-0.6728	-0.7747	-0.7362	-0.7136	-0.8585	-0.8766	-0.6026	-0.9581	-0.6118	-0.6382	-0.625	-0.8033	-0.7637	-0.6976	-0.8958	-0.8165	-0.5524	-0.5193	-0.6358	-0.6698	-0.6811	-0.8057	-0.7604	-0.7038	-0.8623	-0.8057	-0.5792	-0.6698	BCN	19-20	0
881.7	-1.3	-1.3	-1.3	1255.3	-1.3	-1.3	-1.3	5.5	1513.4	-0.6264	-0.6264	-0.6868	-0.8075	-0.7472	-0.6566	-0.8679	-0.8377	-0.566	-0.5358	1126.2	-1.3	-1.3	-1.3	1340.2	-1.3	-1.3	-1.3	12.3	1547.4	BN	19-20	0
936	-1.3	-1.3	-1.3	1333.4	-1.3	-1.3	-1.3	8.9	1516.8	959.8	-1.3	-1.3	-1.3	1241.7	-1.3	-1.3	-1.3	2.1	1544	-0.6566	-0.6264	-0.717	-0.7774	-0.7774	-0.6566	-0.8981	-0.6868	-0.5358	-0.6264	CN	19-20	0
-0.6231	-0.6627	-0.6825	-0.808	-0.7618	-0.7156	-0.8807	-0.8344	-0.5769	-0.9203	-0.6373	-0.6288	-0.6967	-0.7986	-0.7561	-0.7052	-0.8665	-0.858	-0.5608	-0.8156	-0.6742	-0.6187	-0.7138	-0.793	-0.7481	-0.7111	-0.8617	-0.8485	-0.5553	-0.9172	AB	19-20	0
-0.6411	-0.6547	-0.6479	-0.7996	-0.7589	-0.7611	-0.8811	-0.8653	-0.5596	-0.9219	-0.5849	-0.5849	-0.8491	-0.8491	-0.8491	-0.5849	-0.8491	-0.8491	-0.5849	-1.1132	-0.6198	-0.6198	-0.6726	-0.8179	-0.7651	-0.6462	-0.8708	-0.8311	-0.567	-0.7915	ABC	19-20	0
-0.6298	-0.6321	-0.6864	-0.8245	-0.7589	-0.7226	-0.8925	-0.8472	-0.5913	-0.9242	-0.5849	-0.5849	-0.7358	-0.7358	-0.7358	-0.5094	-0.8113	-0.8113	-0.5094	-0.5849	1221.3	-1.3	-1.3	-1.3	518.3	-1.3	-1.3	-1.3	5.5	1547.4	ABN	19-20	0
-0.6234	-0.6355	-0.6868	-0.8075	-0.7592	-0.7502	-0.8891	-0.8649	-0.5419	-0.9162	-0.6557	-0.6715	-0.6926	-0.7719	-0.7481	-0.6979	-0.8617	-0.8617	-0.5843	-0.9145	-0.6127	-0.6608	-0.709	-0.7995	-0.7599	-0.7344	-0.8929	-0.8901	-0.5759	-0.9269	AC	19-20	0
-0.614	-0.6253	-0.6842	-0.7996	-0.7566	-0.7453	-0.8766	-0.8381	-0.58	-0.9355	1211.1	-1.3	-1.3	-1.3	470.8	-1.3	-1.3	-1.3	5.5	1544	-0.6132	-0.6396	-0.6925	-0.7981	-0.7717	-0.6396	-0.9038	-0.8245	-0.5604	-0.5868	ACN	19-20	0
-0.6275	-0.6502	-0.6751	-0.8177	-0.7589	-0.7181	-0.8902	-0.8698	-0.58	-0.9491	-0.6377	-0.6756	-0.6566	-0.8081	-0.7627	-0.7172	-0.8724	-0.8876	-0.5847	-0.8838	-0.6524	-0.6608	-0.7203	-0.791	-0.7571	-0.7429	-0.9099	-0.8476	-0.5816	-0.9184	AN	19-20	0
-0.6292	-0.6662	-0.69	-0.7957	-0.7455	-0.7217	-0.8802	-0.8485	-0.5764	-0.9489	-0.6132	-0.6698	-0.7264	-0.783	-0.783	-0.5566	-0.8396	-0.8396	-0.5566	-0.3302	-0.6604	-0.6226	-0.6981	-0.8113	-0.7736	-0.5472	-0.8868	-0.8491	-0.5094	-0.3585	BC	19-20	0
-0.6108	-0.6345	-0.6794	-0.7957	-0.7481	-0.7138	-0.867	-0.8406	-0.6002	-0.9251	-0.6396	-0.6396	-0.6925	-0.7981	-0.7453	-0.534	-0.8774	-0.7981	-0.534	-0.5604	-0.6085	-0.6745	-0.6745	-0.8066	-0.7406	-0.6085	-0.7406	-0.8066	-0.5425	-0.6745	BCN	19-20	0
769.6	-1.3	-1.3	-1.3	1241.7	-1.3	-1.3	-1.3	2.1	1520.2	-0.5566	-0.6887	-0.8208	-0.6887	-0.6887	0.2358	-0.8208	-0.6887	-0.4245	-0.5566	1058.3	-1.3	-1.3	-1.3	1306.2	-1.3	-1.3	-1.3	8.9	1544	BN	19-20	0
980.2	-1.3	-1.3	-1.3	1296	-1.3	-1.3	-1.3	8.9	1516.8	766.2	-1.3	-1.3	-1.3	1231.5	-1.3	-1.3	-1.3	5.5	1544	-0.6887	-0.6887	-0.6887	-0.6887	-0.6887	-0.0283	-0.8208	-0.8208	-0.5566	-0.6887	CN	19-20	0
-0.5906	-0.6245	-0.6698	-0.8057	-0.7604	-0.6811	-0.8736	-0.8057	-0.5679	-0.8962	-0.6132	-0.6698	-0.7038	-0.8057	-0.7604	-0.6811	-0.9075	-0.8396	-0.5566	-0.8849	-0.6477	-0.6292	-0.6662	-0.7904	-0.756	-0.7138	-0.8723	-0.8485	-0.5711	-0.9013	AB	19-20	0
-0.6398	-0.6874	-0.6345	-0.7851	-0.7613	-0.7111	-0.867	-0.83	-0.5606	-0.9436	-0.5849	-0.8491	-0.5849	-0.5849	-0.8491	-0.3208	-0.8491	-0.8491	-0.5849	-1.1132	-0.5962	-0.6264	-0.6868	-0.7774	-0.7472	-0.3547	-0.8679	-0.8377	-0.566	-0.7472	ABC	19-20	0
-0.6002	-0.6557	-0.6926	-0.7877	-0.7587	-0.7243	-0.8749	-0.8326	-0.5553	-0.9462	-0.4245	-0.5566	-0.6887	-0.8208	-0.8208	-0.1604	-0.6887	-0.6887	-0.5566	-0.6887	1139.8	-1.3	-1.3	-1.3	470.8	-1.3	-1.3	-1.3	5.5	1547.4	ABN	19-20	0
-0.616	-0.633	-0.7009	-0.8085	-0.7632	-0.7236	-0.8764	-0.9047	-0.5368	-0.9443	-0.6398	-0.6319	-0.6583	-0.7957	-0.7534	-0.7191	-0.9225	-0.83	-0.5817	-0.9409	-0.6425	-0.6538	-0.6877	-0.8009	-0.7613	-0.7047	-0.8972	-0.8066	-0.5575	-0.9311	AC	19-20	0
-0.6134	-0.6557	-0.6847	-0.793	-0.7587	-0.7428	-0.8115	-0.8379	-0.5896	-0.9409	1143.2	-1.3	-1.3	-1.3	467.4	-1.3	-1.3	-1.3	5.5	1544	-0.6604	-0.5849	-0.7358	-0.7358	-0.8113	-0.283	-0.8868	-0.8113	-0.5094	-0.2075	ACN	19-20	0
-0.6389	-0.6547	-0.6887	-0.777	-0.7589	-0.7408	-0.8857	-0.8721	-0.5777	-0.9151	-0.5991	-0.671	-0.7467	-0.7921	-0.7618	-0.758	-0.9056	-0.8564	-0.584	-0.8942	-0.6382	-0.6269	-0.6467	-0.7882	-0.7542	-0.7458	-0.8448	-0.8476	-0.5618	-0.8958	AN	19-20	0
-0.6477	-0.5817	-0.7111	-0.7877	-0.7508	-0.7402	-0.8643	-0.8353	-0.5658	-0.9462	-0.5472	-0.6604	-0.6604	-0.7736	-0.7736	0.0189	-0.7736	-0.7736	-0.5472	0.0189	-0.6132	-0.6132	-0.7075	-0.8019	-0.8019	-0.0472	-0.8019	-0.8019	-0.5189	-0.3302	BC	19-20	0
-0.6266	-0.6504	-0.6821	-0.8036	-0.7534	-0.7375	-0.8617	-0.9013	-0.5447	-0.9357	-0.5425	-0.6745	-0.7406	-0.7406	-0.7406	-0.0802	-0.8066	-0.8066	-0.5425	-0.6085	-0.6132	-0.6132	-0.5189	-0.8019	-0.8019	-0.2358	-0.8962	-0.8019	-0.6132	-0.4245	BCN	19-20	0
657.5	-1.3	-1.3	-1.3	1217.9	-1.3	-1.3	-1.3	5.5	1520.2	-0.566	-0.566	-0.566	-0.9434	-0.566	2.0755	-0.566	-0.9434	-0.566	-0.1887	827.4	-1.3	-1.3	-1.3	1279.1	-1.3	-1.3	-1.3	12.3	1547.4	BN	19-20	0
844.3	-1.3	-1.3	-1.3	1282.5	-1.3	-1.3	-1.3	8.9	1516.8	908.9	-1.3	-1.3	-1.3	1207.7	-1.3	-1.3	2.1	12.3	1540.6	-0.566	-0.9434	-0.566	-0.9434	-0.566	2.0755	-0.566	-0.566	-0.566	-0.1887	CN	19-20	0
-0.6132	-0.6396	-0.666	-0.7981	-0.7453	-0.6132	-0.8774	-0.8245	-0.5604	-0.9038	-0.5868	-0.5868	-0.6396	-0.7981	-0.7717	-0.5868	-0.8774	-0.8245	-0.534	-0.8509	-0.6372	-0.5923	-0.6636	-0.8089	-0.7534	-0.7243	-0.8538	-0.8485	-0.5474	-0.9304	AB	19-20	0
-0.6321	-0.6094	-0.6638	-0.7883	-0.7589	-0.7226	-0.8426	-0.8472	-0.5528	-0.9151	-0.4717	-0.4717	-0.4717	-0.8113	-0.8113	0.5472	-0.8113	-0.8113	-0.4717	-1.4906	-0.6274	-0.6274	-0.7123	-0.7123	-0.7972	0.2217	-0.7972	-0.7972	-0.5425	-0.7123	ABC	19-20	0
-0.5845	-0.6117	-0.6615	-0.786	-0.7589	-0.7158	-0.8426	-0.7996	-0.5732	-0.9264	-0.6415	-0.4151	-0.6415	-0.8679	-0.6415	0.2642	-0.6415	-0.4151	-0.4151	0.0377	1126.2	-1.3	-1.3	-1.3	447	-1.3	-1.3	-1.3	5.5	1547.4	ABN	19-20	0
-0.6019	-0.6132	-0.7151	-0.817	-0.7604	-0.6811	-0.8736	-0.783	-0.5453	-0.9189	-0.623	-0.6253	-0.6343	-0.7906	-0.7543	-0.7272	-0.854	-0.8404	-0.6026	-0.9128	-0.6066	-0.6198	-0.6726	-0.8047	-0.7519	-0.6462	-0.884	-0.8311	-0.5538	-0.9236	AC	19-20	0
-0.6298	-0.5913	-0.6932	-0.786	-0.7543	-0.7226	-0.8766	-0.8653	-0.5596	-0.9174	1034.5	-1.3	-1.3	-1.3	464	-1.3	-1.3	-1.3	5.5	1547.4	-0.5755	-0.7453	-0.7453	-0.9151	-0.7453	0.2736	-0.9151	-0.7453	-0.4057	-0.4057	ACN	19-20	0
-0.6162	-0.6955	-0.6932	-0.7951	-0.7589	-0.7272	-0.8472	-0.8449	-0.5574	-0.906	-0.625	-0.6769	-0.7099	-0.8042	-0.7665	-0.7476	-0.875	-0.809	-0.5825	-0.8939	-0.6134	-0.6768	-0.6847	-0.7666	-0.7587	-0.7534	-0.9198	-0.8062	-0.5421	-0.8775	AN	19-20	0
-0.6081	-0.6874	-0.6636	-0.7877	-0.7534	-0.7534	-0.8723	-0.8643	-0.587	-0.9119	-0.6415	-0.8679	-0.6415	-0.6415	-0.6415	1.3962	-0.6415	-0.6415	-0.4151	0.2642	-0.5755	-0.7453	-0.7453	-0.7453	-0.7453	0.9528	-0.7453	-0.7453	-0.4057	-0.066	BC	19-20	0
-0.6134	-0.6953	-0.7455	-0.7772	-0.7534	-0.7349	-0.8406	-0.8775	-0.5579	-0.9172	-0.5755	-0.7453	-0.5755	-0.7453	-0.7453	1.1226	-0.5755	-0.7453	-0.4057	-0.4057	-0.5755	-0.7453	-0.7453	-0.7453	-0.7453	0.4434	-0.7453	-0.9151	-0.5755	-0.4057	BCN	19-20	0
711.9	-1.3	-1.3	2.1	1238.3	-1.3	-1.3	-1.3	2.1	1513.4	0.5189	-0.8019	-0.8019	-0.8019	-0.1415	6.4623	-0.8019	-0.1415	0.5189	-0.1415	773.5	-1.3	-1.3	-1.3	1209	-1.3	-1.3	-1.3	12.5	1544.9	BN	19-20	0

Figure 2: A portion of the dataset

3. Methodology to develop the CANN

3.1 Model Specifications and Development

In the proposed ANN model, two models were combined to develop a combined ANN architecture as a model to best classify both fault type and fault location. The first model, called the 'Up Pyramid," increases the units of the neural network in the order of 32, 128, 512 and 2056 until a final output layer classifies the data. In an ANN, a unit is nothing but a mathematical equation associated with a weight which serves as the most basic building block in a neural network [34]. These increasing layers showed the best experimental results with 'Rectified Linear Unit' or 'ReLu' activation function whose equation is given as per (1) [35] where x is the input variable. This model performs well with classifying fault location but gives only average results while classifying fault type. To improve model performance to identify fault type, the second model reverses the model layout, starting from the layer with 2056 units and building smaller layers until a final output block. This proposed model is termed as 'Down Pyramid' model. This model improves performance on fault type but shows a large drop in accuracy in case of finding fault locations. Thus, to combine the advantages of both the models, a third model is built by combining these two models, called the 'Custom Pyramid' as shown in Figure 3.

$$ReLU = (0, x)_{\max} \tag{1}$$

The first four layers have been termed the "up-pyramid" layers, with increasing units of 32, 128, and 512 respectively. This peaks with a layer called the 'Pyramid Peak," which has 2056 units added as a dense layer on top. The layers are now mirrored downwards with units of 512, 128, and 32, which are termed the 'Down-Pyramid' layers. The input layer accepts 32 input features corresponding to the 32 features in the dataset while the output layer has 28 or 10 features for classification of fault position or fault type respectively. Thus, the ANN is forming a sequential model on which a final output layer is added with a softmax activation function for multiclass classification as shown in (2) where xi is the input value for the i^{th} vector and xj is the input for the j^{th} vector. In addition to this, dropout layers (0.2) are added to minimise overfitting and improve experimental results [36]. Dropout layers work by randomly selecting 20% of the input layers for training. This percentage was selected through experimentation. The network uses the Adam optimizer with a learning rate of 0.0001 to minimise losses and uses categorical crossentropy as its loss function as shown in (3) where p is the prediction made by the model and q is the true label.

$$Softmax(xi) = \frac{e^{xi}}{\sum_j e^{xj}} \tag{2}$$

$$H(p, q) = -\sum_{x \in classes} p(x) \log q(x) \tag{3}$$

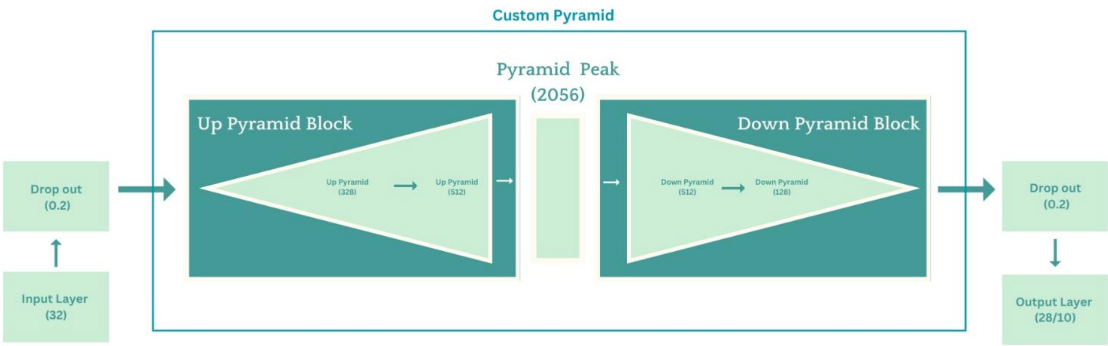

Figure 3: CANN architecture

The computational complexity of the CANN is directly dependent on the number of epochs. Hence, to find the optimal number of epochs, the model is trained up to 1300 epochs and its accuracy curves are plotted in Figure 4, with losses plotted at every 65 epochs to better illustrate the decrease in loss over epoch time. It can be seen from the figure that after 1000 epochs, the accuracies remain almost constant. Thus, 1000 epochs are considered for the proposed CANN. The complete specifications of the architecture of this model is given in Table 1. The first column represents layer name, the second represents the shape of the input that the layer is designed to process while the third column represents the number of parameters which are calculated by the model itself over a training epoch. A comparison of the performance of all three pyramid models is given in Figure 5 which shows that the customised pyramid ANN architecture works better than the up-pyramid as well as the down-pyramid ANN architecture both for fault types as well as fault locations.

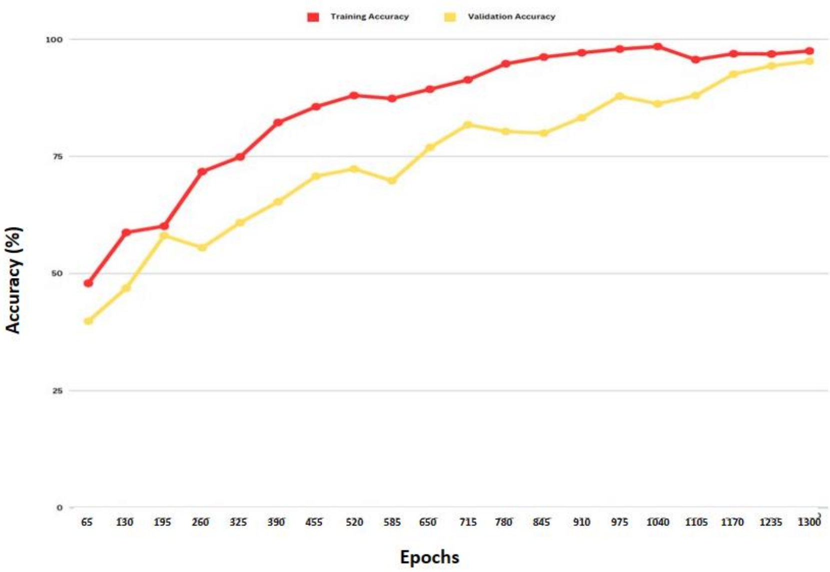

Figure 4: Variation of accuracy with number of epochs

Table 1: Specifications of the architecture of the CANN

Layer (type)	Output Shape	Param #
Input_layer	(None, 32)	992
dropout (Dropout)	(None, 32)	0
Up-Pyramid1	(None, 128)	4224
dropout_1 (Dropout)	(None, 128)	0
Up-Pyramid2	(None, 512)	66048
dropout_2 (Dropout)	(None, 512)	0
Pyramid-Peak	(None, 2056)	1054728
dropout_3 (Dropout)	(None, 2056)	0
Down-Pyramid2	(None, 512)	1053184
dropout_4 (Dropout)	(None, 512)	0
Down-Pyramid1	(None, 128)	65664
dropout_5 (Dropout)	(None, 128)	0
output_layer	(None, 30)	3870

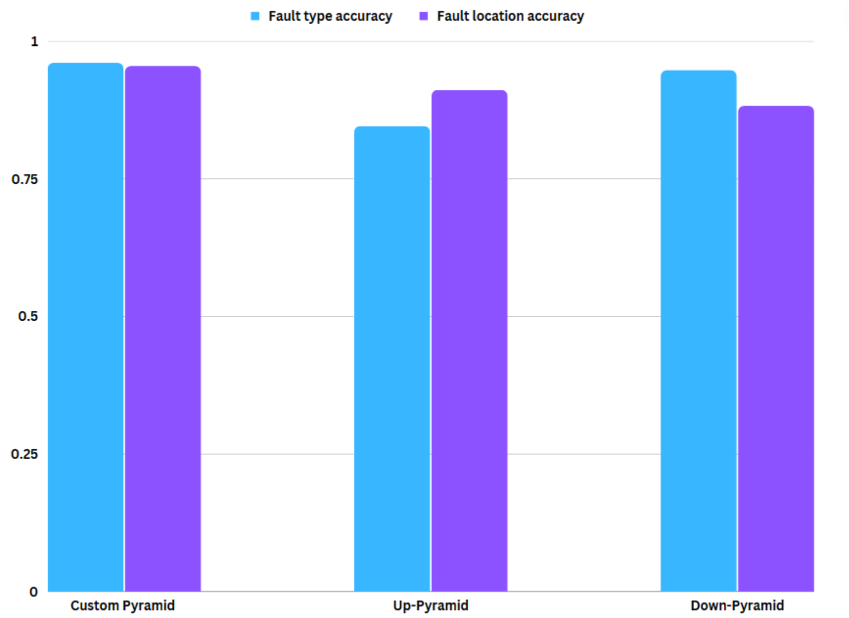

Figure 5: Comparison of the performance of all three pyramid models

3.2 Improving model efficiency by reducing features

The computational complexity is also directly dependent on the number of input features. It is always advisable to reduce the number of features without compromising the performance of a ML model. To achieve this, accuracy is obtained considering all the input features except one at a time and the accuracy is plotted in Figure 6. For example, the accuracy corresponding to IA0 in the x-axis represents the accuracy obtained by the classifier without considering IA0. A similar explanation follows for other features. The corresponding features which reduces the accuracy when not considered are the most important input parameters. After several trial and error, a threshold accuracy of 90% is set as shown in the figure. As a result, the number of features was reduced from the original number of 30 to 15 most important features. Hence, as seen in Figure 6, the features IA2, IA4, IA5, IA7, IB2, IB3, IB6, IB7, IB9, IC0, IC1, IC5, IC6, IC7, IC9 are the important features selected for the network. Every one of the proposed models is trained for 1000 epochs, as it is observed that there is no change in observed accuracy either on the training set or the validation set when increasing the model epochs beyond this point.

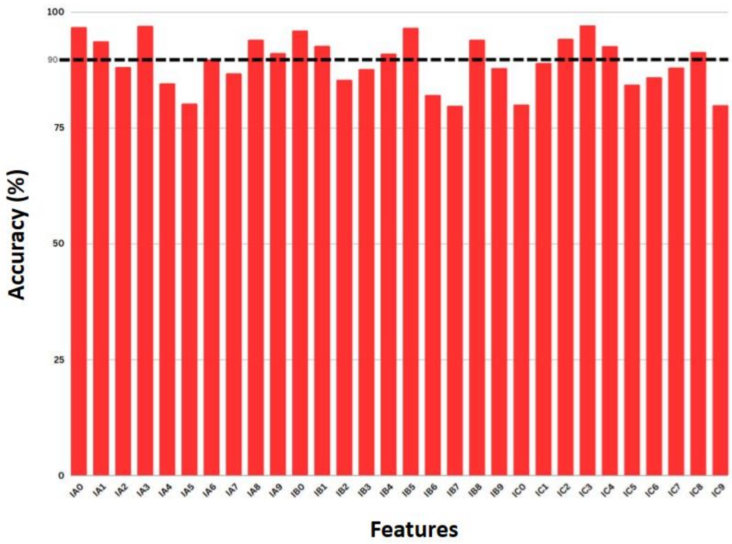

Figure 6: Reduction of features

4. Performance and Results

4.1 Fault type classification

The accuracy of the custom ANN is first compared with various classical ML models for the classification of fault types. Logistical regression (LR) gives an accuracy of 45.45%, KNN performs classification at 75.401%, SVM classifies at 51.06%, DT at 83.16% and random forest (RF) classifies different fault types with an accuracy of 93.04%. It is also evident that the features of IB7, IB8, IC0 were especially important when analysing fault types as their exclusion drops the accuracy to as low as 81%. The custom neural network outperforms these standard ML models by classifying fault types with an accuracy of 96.03%. Figure 7 displays how the custom ANN has very high classification accuracy and compares classification metrics of precision, recall, and F1 score with other classifiers as per (4)-(6), where $\check{t}$ = true positives, $\tilde{t}$ = false positives, $\breve{n}$ = true negatives and $\tilde{n}$= false negatives [37]-[38]. Table 2 shows how the ANN can classify each fault, with single-line to ground faults being accurately identified with the highest accuracy. The model found most success classifying CN, BN, and CN faults, while it performed most poorly on ABC and BCN faults. Upon testing the proposed model on the test set it was seen that classification accuracy of 96.03% is observed as indicated by the confusion matrix in Figure 8. The confusion matrix allows visualization of tested data where the predictions are on the vertical axis while the ground truth is on the horizontal axis.

$$Precision = {\check{t}}/{\tilde{t} + \check{t}} \tag{4}$$

$$Recall = {\check{t}}/{\tilde{n} + \check{t}} \tag{5}$$

$$F1\ score = \frac{2 \times Precision \times Recall}{Precision + Recall} \tag{6}$$

Table 2: Performance of CANN for fault type classification

Number	Fault Type	Precision	Recall	F1 Score
0	AB	0.96	0.99	0.98
1	ABC	0.95	0.92	0.94
2	ABN	0.98	0.98	0.98
3	AC	0.97	0.98	0.98
4	ACN	1	0.98	0.99
5	AN	0.98	0.95	0.96
6	BC	0.93	0.95	0.94
7	BCN	0.95	0.92	0.94
8	BN	0.99	0.99	0.99

9	CN	0.99	0.99	0.99

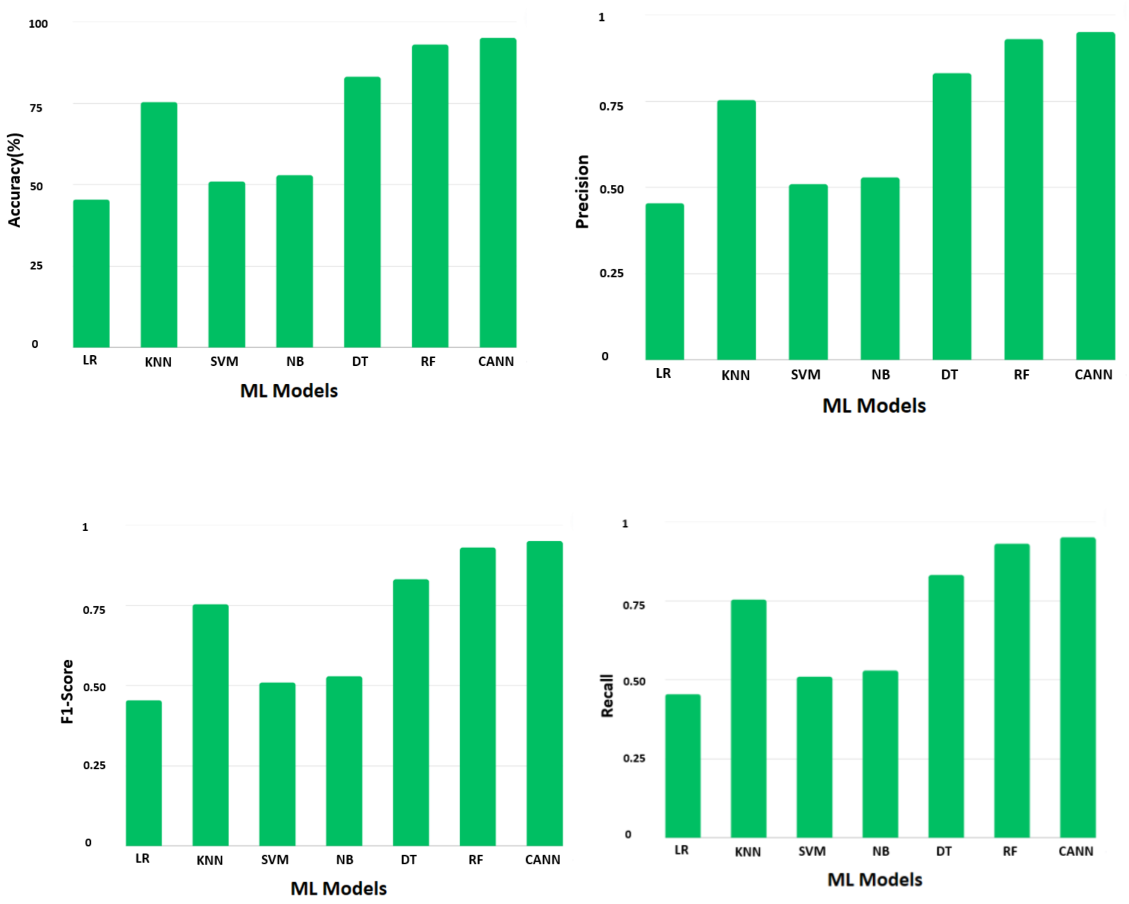

Figure 7: Comparison of CANN with other ML methods for fault type classification

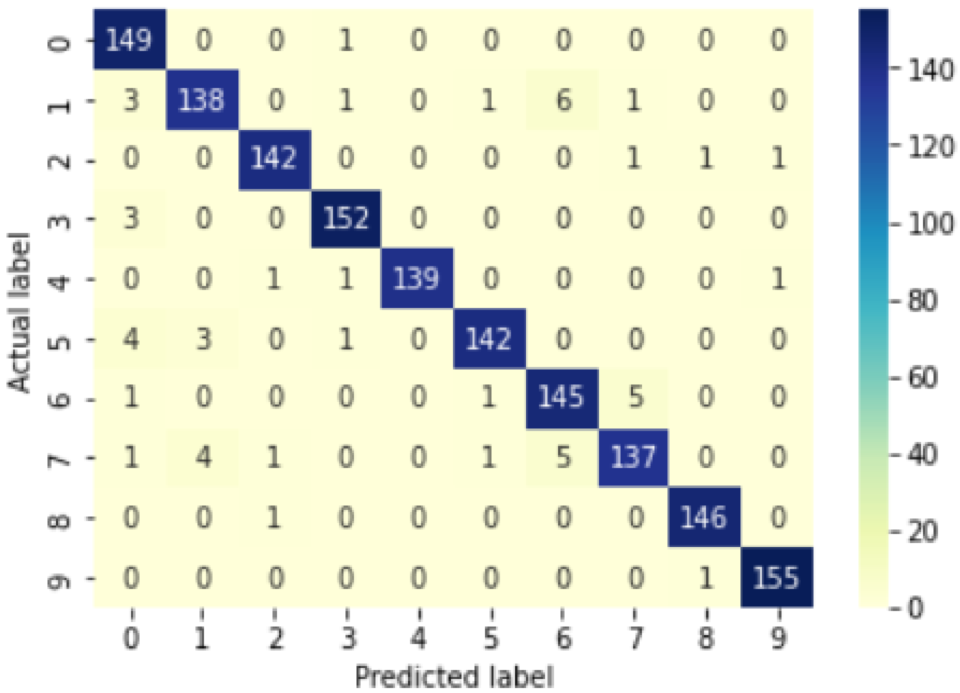

Figure 8: Confusion matrix for fault type classification

4.2 Fault positions classification

The dataset contains simulated samples of 28 different total fault positions in the sample IEEE bus system. The dataset is tested using traditional ML algorithms. Out of these, LR can classify fault positions with an accuracy of 30.75%. KNN identifies position with an accuracy of 64.17%, SVM performs at 31.55%, Naïve Bayes (NB) classifies position at 47.05%, and DT and RF performs slightly better, categorising simulated data with accuracies of 67.647% and 81.01%, respectively. The dataset is now tested on the custom ANN. The custom ANN classifies fault positions with a significantly higher accuracy of 95.43%, and its accuracy at each fault position is shown in Table 3. It can be seen from the table that the method works best for fault between bus 19-20, 20-21 and13-14 and worst for bus11-12. Figure 9 shows a comparison between the ANN and standard ML models where the classification metrics of precision, recall, and F1 score with other classifiers are calculated as per (4)-(6). The model is tested on a similar test set where samples are shuffled to prevent overfitting. It is observed that the model still performs at accuracies of over 95%, which are given in Figure 10 as its confusion matrix, which establishes its high efficiency in identifying fault positions.

Table 3: Performance of CANN for fault location classification

Number	From--To	Precision	Recall	F1 Score
0	19--20	0.97	1	0.98
1	20--21	1	0.93	0.97
2	27--28	0.88	0.95	0.91
3	29--30	0.93	0.85	0.89
4	28--29	0.83	0.98	0.9
5	26--27	0.9	0.92	0.91
6	15--16	0.9	0.91	0.9
7	8 --9	0.93	0.91	0.92
8	21--8	0.94	0.9	0.92
9	13--14	0.98	1	0.99
10	7--26	0.94	0.96	0.95
11	6--7	0.98	0.93	0.95
12	5--6	0.92	0.94	0.93
13	4--5	0.89	0.91	0.9
14	3--4	0.98	0.92	0.95
15	0--2	0.96	0.96	0.96
16	2--3	0.89	0.93	0.91
17	24--25	0.95	0.93	0.94
18	23--24	0.96	0.92	0.94
19	3--23	0.98	0.96	0.86
20	18--33	0.91	0.92	0.92
21	17--18	0.98	0.92	0.95
22	16--17	0.89	0.85	0.87
23	12--13	1	0.98	0.99
24	11--12	0.92	0.69	0.79
25	10--11	0.81	0.85	0.83
26	22--12	0.94	0.96	0.95
27	21--22	0.96	0.94	0.95

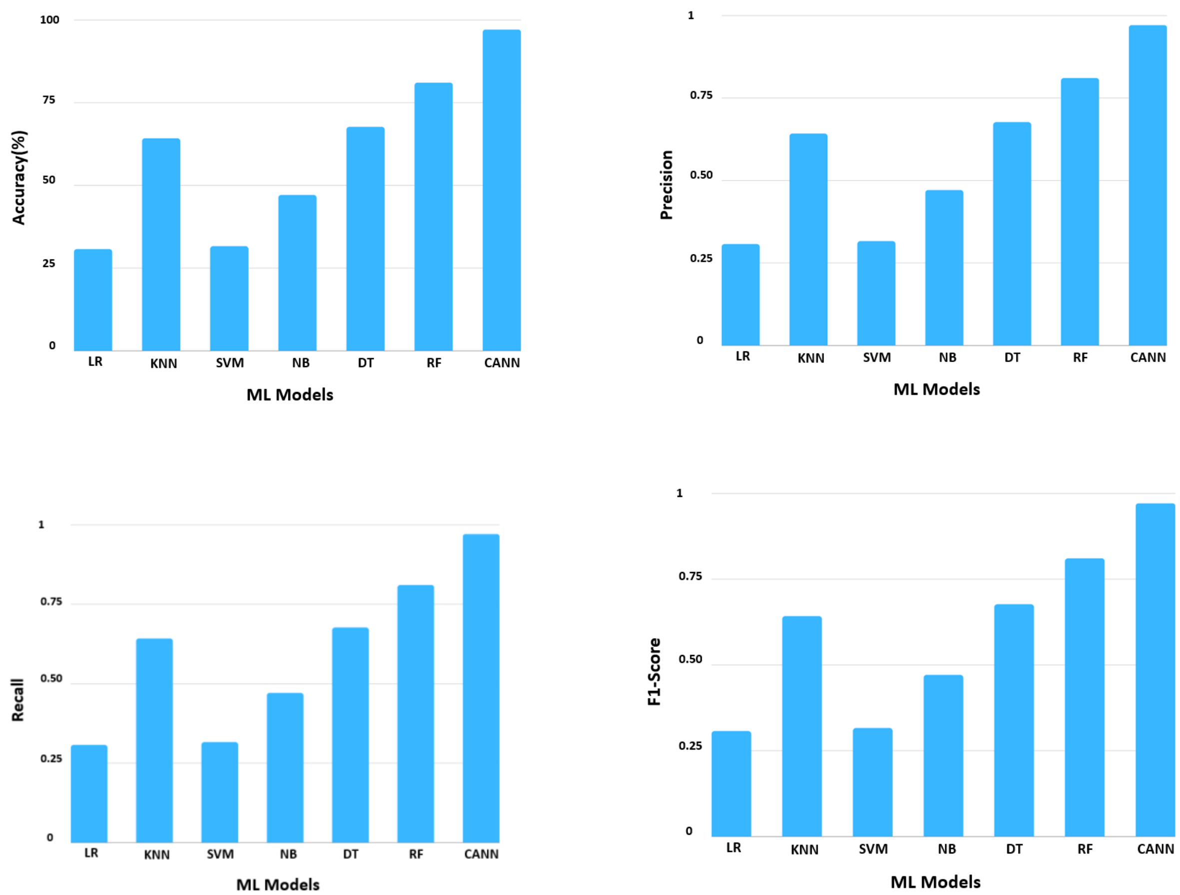

Figure 9: Comparison of CANN with other ML methods for fault location classification

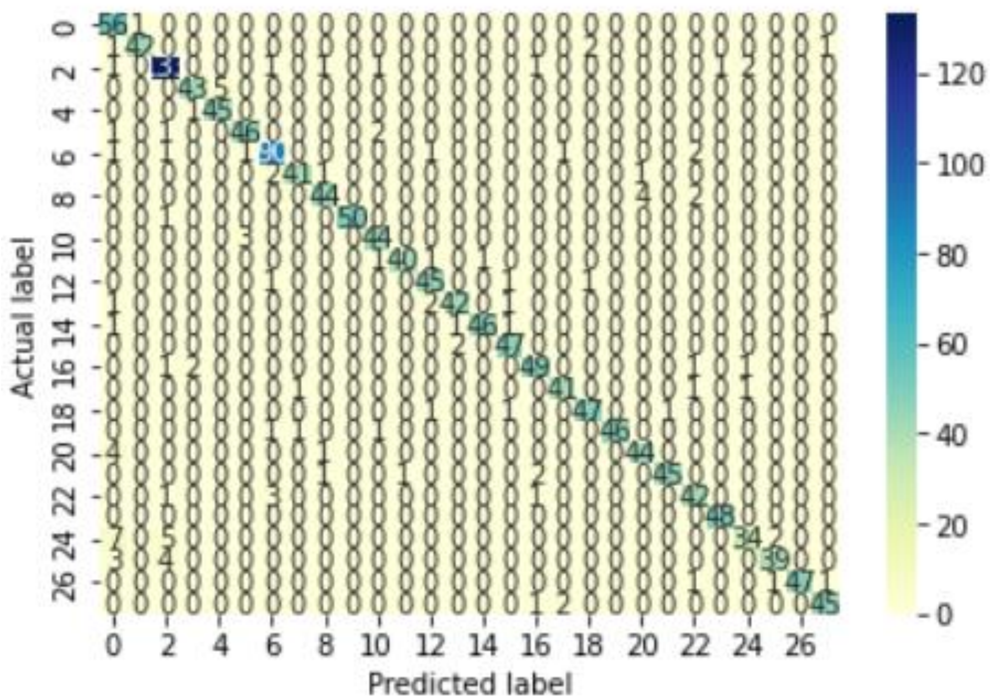

Figure 10: Confusion matrix for fault location classification

4.3 Results for different out of the box scenarios

The proposed model is tested against some out of the sample dataset i.e. the conditions that are not considered in the training or testing data. For this, several types of faults at different locations is simulated with different fault inception angle and fault resistances and the results are tabulated in Table 4. It can be seen that the proposed algorithm works perfectly for all cases except the cases for high impedance fault i.e. when the fault resistance exceeds 200Ω and when the fault inference angle exceeds 330°. For further analysing the model, several scenarios are simulated considering Gaussian noise at various levels. The results for different noise levels in dB is shown in Table 5. It can be seen from the table that the method is able to classify the faults and its locations up to 30dB of noise.

Table 4: Performance of CANN for different fault inference angles and fault resistances

Description of cases	CANN output for fault type	CANN output for fault location
AB fault between node 6 and 7 with 22Ω fault resistance and 37° fault inference angle	AB (Correct)	6--7 (Correct)
BCG fault between node 12 and 22 with 68Ω fault resistance and 72° fault inference angle	BCG (Correct)	22--12 (Correct)
AG fault between node 28 and 29 with 92Ω fault resistance and 184° fault inference angle	AG (Correct)	28--29 (Correct)
ACG fault between node 11 and 12 with 156Ω fault resistance and 228° fault inference angle	ACG (Correct)	11--12 (Correct)
BG fault between node 18 and 33 with 187Ω fault resistance and 339° fault inference angle	AG (Incorrect)	18--33 (Correct)
AB fault between node 23 and 24 with 220Ω fault resistance and 350° fault inference angle	CG (Incorrect)	3--23 (Incorrect)

Table 5: Performance of CANN for different noise levels

Description of cases	CANN output for fault type	CANN output for fault location
ACG fault between node 15 and 16 with 5 dB noise	ACG (Correct)	15--16 (Correct)
AG fault between node 17 and 18 with 10 dB noise	AG (Correct)	17--18 (Correct)
CG fault between node 26 and 27 with 15 dB noise	CG (Correct)	26--27 (Correct)
ABG fault between node 8 and 21 with 20 dB noise	ABG (Correct)	21--8 (Correct)
BC fault between node 6 and 7 with 30 dB noise	BC (Correct)	7--26 (Incorrect)
BCG fault between node 26 and 27 with 40 dB noise	AB (Incorrect)	27--28 (Incorrect)

4.4 Results for another dataset

The proposed model is tested on other microgrid situations such as for Vehicle-to-Grid communication channel selection. The simulated microgrid is simulated in a 33 bus microgrid system which is tested against the charging and transport capabilities of electrical vehicles. Various parameters of electrical vehicles are simulated against the system and estimated battery type is to be predicted using the proposed model. However, its accuracy does not exceed 54% on the tested data while making predictions on fuel usage forecast, while performing at 38.3% for predictions on closest bus, making the proposed CANN model highly application specific.

4.5 Comparison with other techniques

The greatest advantage of the proposed technique is its ability to detect both fault types as well as fault locations with a single model. This reduces the computational complexity which is other otherwise significant if separate algorithms are used for determining fault types and fault locations. This reduction in complexity will help in reducing the software and hardware cost. It has the advantage of high speed when compared with traditional techniques, no problem of threshold settings when compared with signal processing techniques, no requirement of an expert's knowledge when compared with knowledge-based techniques and a common algorithm both for fault types classification as well as fault location estimation when compared with other ML techniques. The CANN technique has been compared with other techniques in Table 6.

Table 6: Comparison of CANN with other techniques

Techniques	Advantage	Disadvantage
Traditional	Simple procedure	Slow with limited ability of fault classification
Signal processing	Faults are diagnosed directly	Very difficult to ascertain the thresholds
Knowledge based	Low chances of misclassification	Massively relies on the knowledge of the professional
ML	Less heuristics	No common algorithms both for fault types classification as well as fault location estimation
CANN	Common algorithm both for fault types classification as well as fault location estimation.	Highly application specific

5. Conclusions

The proposed work develops a CANN that combines the "up-pyramid" and "down-pyramid" model of ANN into a "custom-pyramid" model. As a result, the same model can be used both for determining the types of fault as well as its location. Since, the CANN model was complex and large in size initially, an additional scope of improvement was seen in reduction of model complexity by further analysing important classification features like IB7, IB8 or IC0. Thus, the paper also showcases how the reduction of input features reduces computational complexity without compromising its accuracy. The proposed ANN model classifies fault location with an accuracy of 95.43% which is significantly higher than previous traditional ML algorithms which are to a maximum of 81.01% on the tested data. The proposed ANN also identified precise fault type with an accuracy of 96.08% which outperforms traditional algorithms which peak at 93.04%. The proposed model is also tested on other microgrid situations such as for Vehicle-to-Grid communication channel selection where it performed poorly. Proposed model was hence found to be highly application specific in its usage. Further, the algorithm is tested against various out of sample dataset such as different fault resistance, fault inference angles and noise levels. The model gave satisfactory output with some limitations.

There is considerable scope of improvement in identifying correct fault position especially when the fault is between nodes 11 and 12 where accuracy is only at 79% and while identifying ABC type faults which are identified only at an accuracy of 94%. Performance of the model can also be improved by the availability of a larger dataset either by simulation or larger augmented data. Future modification of the model can involve improvement in classification of selected data cases where the proposed model performs worse than its mean.

References

[1] Burger SP, Jenkins JD, Batlle C., Pérez-Arriaga I. J. Restructuring revisited part 1: Competition in electricity distribution systems. The Energy Journal. 2019. 40.

[2] Srikanth P, Koley C. Fuzzified time-frequency method for identification and localization of power system faults. Journal of Intelligent & Fuzzy Systems. 2022; 42:1027-1039.

[3] Gatta FM, Geri A, Lauria S, Maccioni M. Analytical prediction of abnormal temporary overvoltages due to ground faults in MV networks. Electric power systems research. 2007; 77:1305-1313.

[4] Muir A, Lopatto J. Final report on the August 14, 2003 blackout in the United States and Canada: causes and recommendations.

[5] Ruester S, Schwenen S, Batlle C, Pérez-Arriaga I. From distribution networks to smart distribution systems: Rethinking the regulation of European electricity DSOs. Utilities Policy. 2014 Dec 1;31:229-37.

[6] Georgilakis PS, Hatziargyriou ND. A review of power distribution planning in the modern power systems era: Models, methods and future research. Electric Power Systems Research. 2015 Apr 1;121:89-100.

[7] Avancini DB, Rodrigues JJ, Martins SG, Rabêlo RA, Al-Muhtadi J, Solic P. Energy meters evolution in smart grids: A review. Journal of cleaner production. 2019 Apr 20;217:702-15.

[8] Lin S, et al. Travelling wave time-frequency characteristic-based fault location method for transmission lines. Gener Transm Distrib IET 2012;6:764–72.

[9] Lopes FV, et al. Real-time traveling-wave-based fault location using two-terminal unsynchronized data. IEEE Trans Power Deliv 2015;30:1067–76.

[10] Sant MT, Paithankar YG. Online digital fault locator for overhead transmission line. Electr Eng Proc Inst of 1979;126:1181–5.

[11] Choi M-S, et al. A new fault location algorithm using direct circuit analysis for distribution systems. Power Deliv IEEE Trans 2004;19:35–41.

[12] Brahma SM. Fault location in power distribution system with penetration of distributed generation. IEEE Trans Power Deliv 2011;26:1545–53.

[13] Sharma NK, Samantaray SR. Assessment of PMU-based wide-area angle criterion for fault detection in microgrid. IET Generation, Transmission & Distribution. 2019 Aug 1;13(19):4301-10.

[14] Dehghani, M., Khooban, M.H., Niknam, T.: 'Fast fault detection and classification based on a combination of wavelet singular entropy theory and fuzzy logic in distribution lines in the presence of distributed generations', Int. J. Electr. Power Energy Syst., 2016, 78, pp. 455–462.
[15] Samantaray, S.R., Joos, G., Kamwa, I..: 'Differential energy based microgrid protection against fault conditions'. IEEE PES Innovative Smart Grid Technologies (ISGT), 2012, pp. 1–7
[16] Kar, S., Samantaray, S.R..: 'Time–frequency transform-based differential scheme for microgrid protection', IET Gener. Transm. Distrib., 2014, 8, pp. 310–320.
[17] Anand A, Affijulla S. Hilbert-Huang transform based fault identification and classification technique for AC power transmission line protection. International Transactions on Electrical Energy Systems. 2020 Oct;30(10):e12558.
[18] Kavi M, Mishra Y, Vilathgamuwa MD. High-impedance fault detection and classification in power system distribution networks using morphological fault detector algorithm. IET Generation, Transmission & Distribution. 2018 Aug 16;12(15):3699-710.
[19] Pradhan AK, et al. Higher order statistics-fuzzy integrated scheme for fault classification of a series-compensated transmission line. IEEE Trans Power Deliv 2004;19:891–3.
[20] Das B, Reddy JV. Fuzzy-logic-based fault classification scheme for digital distance protection. IEEE Trans Power Deliv 2005;20:609–16.
[21] Das B. Fuzzy logic-based fault-type identification in unbalanced radial power distribution system. IEEE Trans Power Deliv 2006;21:278–85.
[22] Adhikari NS Shuma, Dorendrajit Thingam. Fuzzy logic based on-line fault detection and classification in transmission line. Springerplus 2016;5.
[23] Cardoso G, Jr., et al. Application of neural-network modules to electric power system fault section estimation. Power Deliv IEEE Trans on 2004;19:1034–41.
[24] Bretas A, et al. A BP neural network based technique for HIF detection and location on distribution systems with distributed generation. In: Huang D-S, editor. .Computational intelligence, 4114. Berlin Heidelberg: Springer; 2006. p. 608–13.
[25] Zavadian SAM, , et al. Determining fault's type and accurate location in distribution systems with DG using MLP neural networks. In: Proceedings of the clean electrical power, 2009 international conference on. 2009, p. 284–9.
[26] Koley E, et al. An improved fault detection classification and location scheme based on wavelet transform and artificial neural network for six phase transmission line using single end data only. Springerplus 2015;4:551.
[27] Salat R, Osowski S. Accurate fault location in the power transmission line using support vector machine approach. IEEE Trans Power Syst 2004;19:979–86.
[28] Janik P, Lobos T. Automated classification of power-quality disturbances using SVM and RBF networks. IEEE Trans Power Deliv 2006;21:1663–9.
[29] Ekici S. Support vector machines for classification and locating faults on transmission lines. Appl Soft Comput 2012;12:1650–8.
[30] Deng X, et al. Fault location in loop distribution network using SVM technology. Int J Electr Power Energy Syst 2015;65:254–61.
[31] Godse, R., Bhat, S., 2020. Mathematical morphology-based feature-extraction technique for detection and classification of faults on power transmission line. IEEE Access 8, 38459–38471.
[32] Asadi Majd, A., Samet, H. & Ghanbari, T. k-NN based fault detection and classification methods for power transmission systems. Prot Control Mod Power Syst 2, 32 (2017).
[33] Sahu, S. K., Roy, M., Dutta, S., Ghosh, D., & Mohanta, D. K. (2023). Machine learning based adaptive fault diagnosis considering hosting capacity amendment in active distribution network. Electric Power Systems Research, 216, 109025.
[34] Dutta, S., Sadhu, P. K., Cherikuri, M., & Mohanta, D. K. (2022). Application of Artificial Intelligence and Machine Learning Techniques in Island Detection in a Smart Grid. Intelligent Renewable Energy Systems, 79-109.
[35] Hara, K., Saito, D., & Shouno, H. (2015, July). Analysis of function of rectified linear unit used in deep learning. In 2015 international joint conference on neural networks (IJCNN) (pp. 1-8). IEEE.
[36] Srivastava, N., Hinton, G., Krizhevsky, A., Sutskever, I., & Salakhutdinov, R. (2014). Dropout: a simple way to prevent neural networks from overfitting. The journal of machine learning research, 15(1), 1929-1958.
[37] Dutta, S., Sahu, S. K., Dutta, S., & Dey, B. (2022). Leveraging a micro synchrophasor for fault detection in a renewable based smart grid—A machine learned sustainable solution with cyber-attack resiliency. e-Prime-Advances in Electrical Engineering, Electronics and Energy, 2, 100090.
[38] Goutte, C., & Gaussier, E. (2005). A probabilistic interpretation of precision, recall and F-score, with implication for evaluation. In Advances in Information Retrieval: 27th European Conference on IR Research, ECIR 2005, Santiago de Compostela, Spain, March 21-23, 2005. Proceedings 27 (pp. 345-359). Springer Berlin Heidelberg.

CRediT authorship contribution statement

Arnav Bhagwat: Methodology, Software, Writing – original draft. **Soham Dutta:** Conceptualization, Methodology, Investigation, Writing – original draft. **Vinay Kumar Jadoun**: Conceptualization, Methodology. **Sourav Kumar Sahu:** Writing – original draft, Writing – review & editing. **Arigela Sri Satya Veerendra Babu**: Investigation, Writing – review & editing, Supervision.

Declaration of Competing Interest

The authors declare that they have no known competing financial interests or personal relationships that could have appeared to influence the work reported in this paper.

Data availability

Data will be made available on request.

Declaration of interests

☒The authors declare that they have no known competing financial interests or personal relationships that could have appeared to influence the work reported in this paper.

☐The authors declare the following financial interests/personal relationships which may be considered as potential competing interests:

- All persons who meet authorship criteria are listed as authors, and all authors certify that they have participated sufficiently in the work to take public responsibility for the content, including participation in the concept, design, analysis, writing, or revision of the manuscript. Furthermore, each author certifies that this material or similar material has not been and will not be submitted to or published in any other publication before its appearance.

- **Authors' contributions: Arnav Bhagwat:** Methodology, Software, Writing – original draft. **Soham Dutta:** Conceptualization, Methodology, Investigation, Writing – original draft. **Vinay Kumar Jadoun:** Conceptualization, Methodology. **Sourav Kumar Sahu:** Writing – original draft, Writing – review & editing. **Arigela Sri Satya Veerendra Babu:** Investigation, Writing – review & editing, Supervision.